Supplementary Information

Structural Stabilities, Elastic Property, and Robust Topological Phases in Janus $MoWCO_2$ MXene from First-Principles Investigation

Sirinee Thasitha[a], Prutthipong Tsuppayakorn-aek[b], Thanayut Kaewmaraya[c,d], Tanveer Hussain[e], Thiti Bovornratanaraks[f] and Komsilp Kotmool[a,g,*]

[a]School of Integrated Innovative Technology, King Mongkut's Institute of Technology Ladkrabang, Bangkok 10520, Thailand.

[b]Division of Physics, Faculty of Science and Technology, Princess of Naradhiwas University, Narathiwat, 96000, Thailand

[c]Integrated Nanotechnology Research Center, Department of Physics, Khon Kaen University, Khon Kaen, Thailand.

[d]Institute of Nanomaterials Research and Innovation for Energy (IN-RIE), NANOTEC-KKU RNN on Nanomaterials Research and Innovation for Energy, Khon Kaen University, Khon Kaen, 40002, Thailand.

[e]School of Science and Technology, University of New England, Armidale, New South Wales 2351, Australia.

[f]Extreme Conditions Physics Research Laboratory and Center of Excellence in Physics of Energy Materials (CE:PEM), Department of Physics, Faculty of Science, Chulalongkorn University, Bangkok 10330, Thailand.

[g]School of Science, King Mongkut's Institute of Technology Ladkrabang, Bangkok 10520, Thailand

[*]*Electronic mail:* komsilp.ko@kmitl.ac.th

Table S1. The crystal lattice parameter *a*, layer thickness (*d*), and relative energy (Δ*E*) of the 2 H and 1 T phases of Janus MoWC with O terminations at different surface positions were determined through optimization.

Position of O-termination	**Phase**	***a* = *b***	***d***	**Δ*E***	**Phase**	***a* = *b***	***d***	**Δ*E***
		Å	**Å**	**meV/atom**		**Å**	**Å**	**meV/atom**
A-A'	2H	2.88	6.70	0	1T	2.88	6.67	98
A-B'	2H	2.93	7.23	160	1T	2.90	6.63	454
A-C'	2H	2.89	6.70	440	1T	2.95	7.11	274
B-B'	2H	2.99	7.81	219	1T	3.12	6.58	454
B-A'	2H	2.92	7.24	125	1T	2.96	7.07	239
B-C'	2H	2.94	7.24	544	1T	3.14	7.32	312
C-C'	2H	2.90	6.70	850	1T	3.11	6.64	446
C-A'	2H	2.90	6.68	423	1T	2.91	6.59	438
C-B'	2H	2.95	7.21	546	1T	3.10	5.94	664

Table S2. Comparison of elastic constants (C_{ij}) and in-plane shear modulus (G^{2D}) of 2H- and 1T-$MoWCO_2$ phases, with and without SOC.

Model	**nSOC**				**SOC**		
	C_{11}=C_{22}	**C_{12}**	**C_{55}=C_{66}**	**G^{2D}**	**C_{11}**	**C_{12}**	**G^{2D}**
	$N \cdot m^{-1}$	$N \cdot m^{-1}$	$N \cdot m^{-1}$	$N \cdot m^{-1}$	$N \cdot m^{-1}$	$N \cdot m^{-1}$	$N \cdot m^{-1}$
2H-$MoWCO_2$	449.649	176.002	178.083	136.823	449.940	173.680	138.130
1T-$MoWCO_2$	418.320	198.700	133.391	109.810	424.487	189.239	117.624

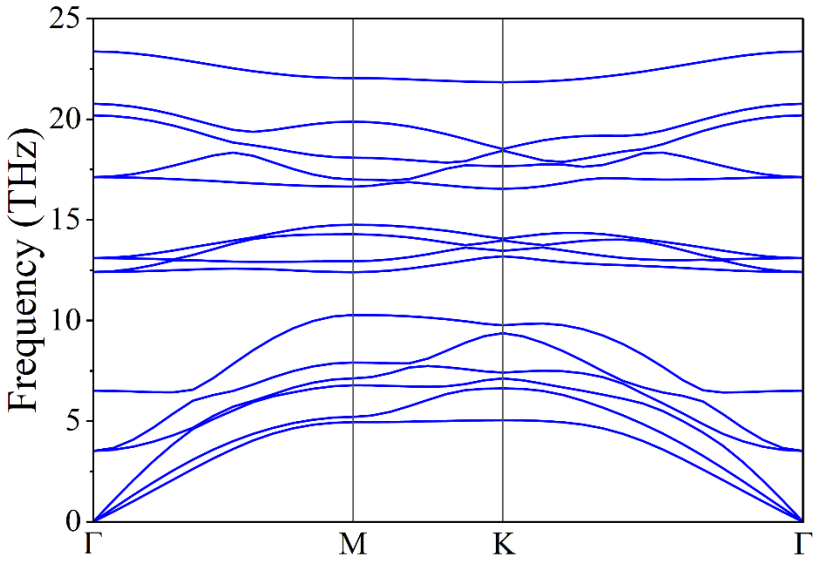

Figure S1. Phonon dispersion curve of the 1T-$MoWCO_2$ phase without SOC.

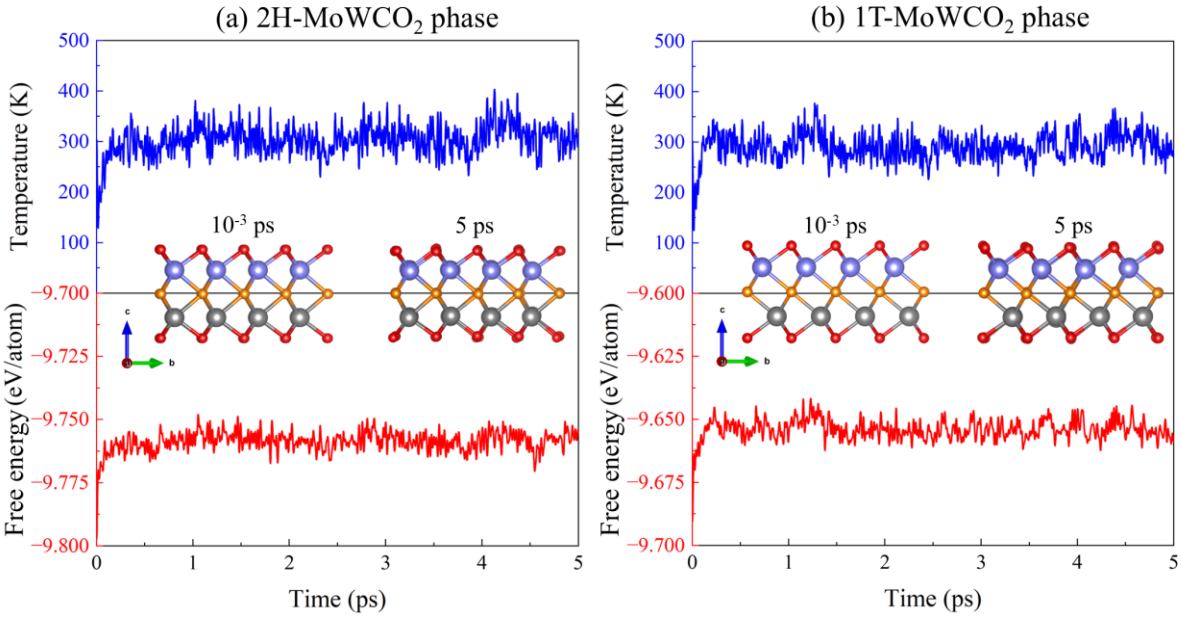

Figure S2. The AIMD simulations of Janus $MoWCO_2$ in the (a) 2H and (b) 1T phases performed at 300 K. The time evolution of the temperature (upper) and free energy per atom (lower) is shown over a simulation duration of 5 ps. The inset atomic structures compare the initial configurations with the final structures.

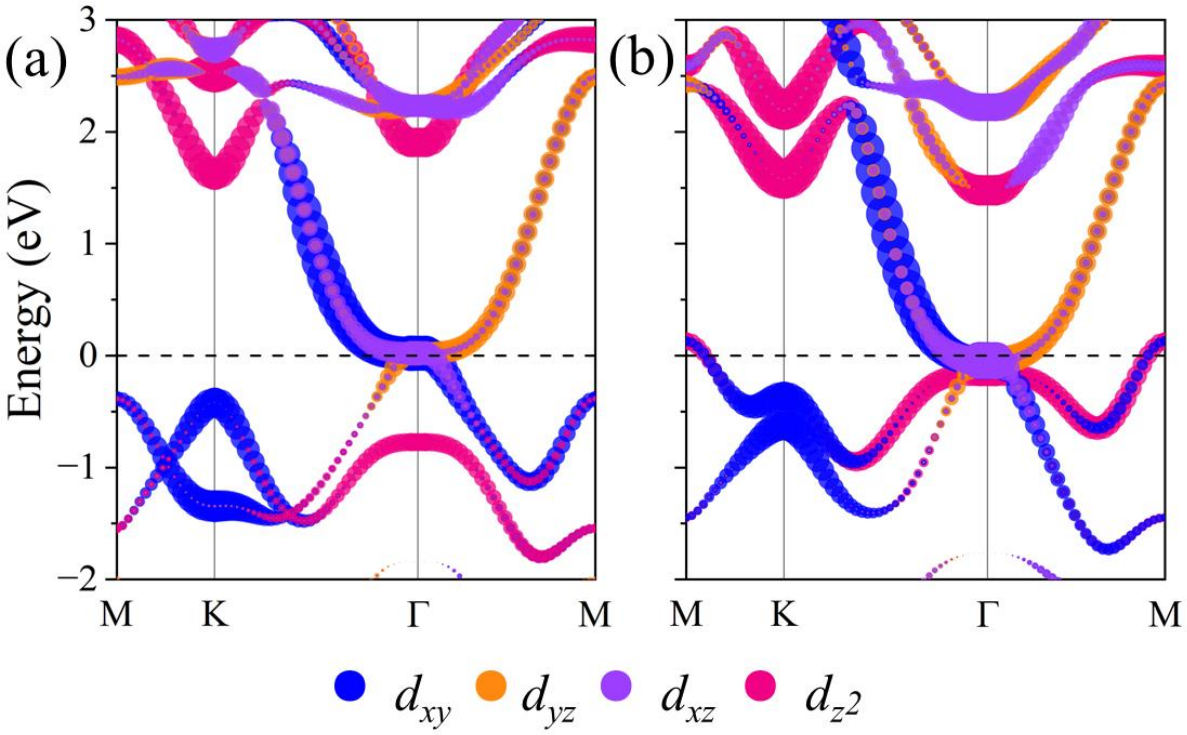

Figure S3. Electronic band structures of the (a) 2H and (b) 1T phases of $MoWCO_2$ calculated without SOC. The fat bands are weighted by the projected contributions of different atomic orbitals to the eigenstates.

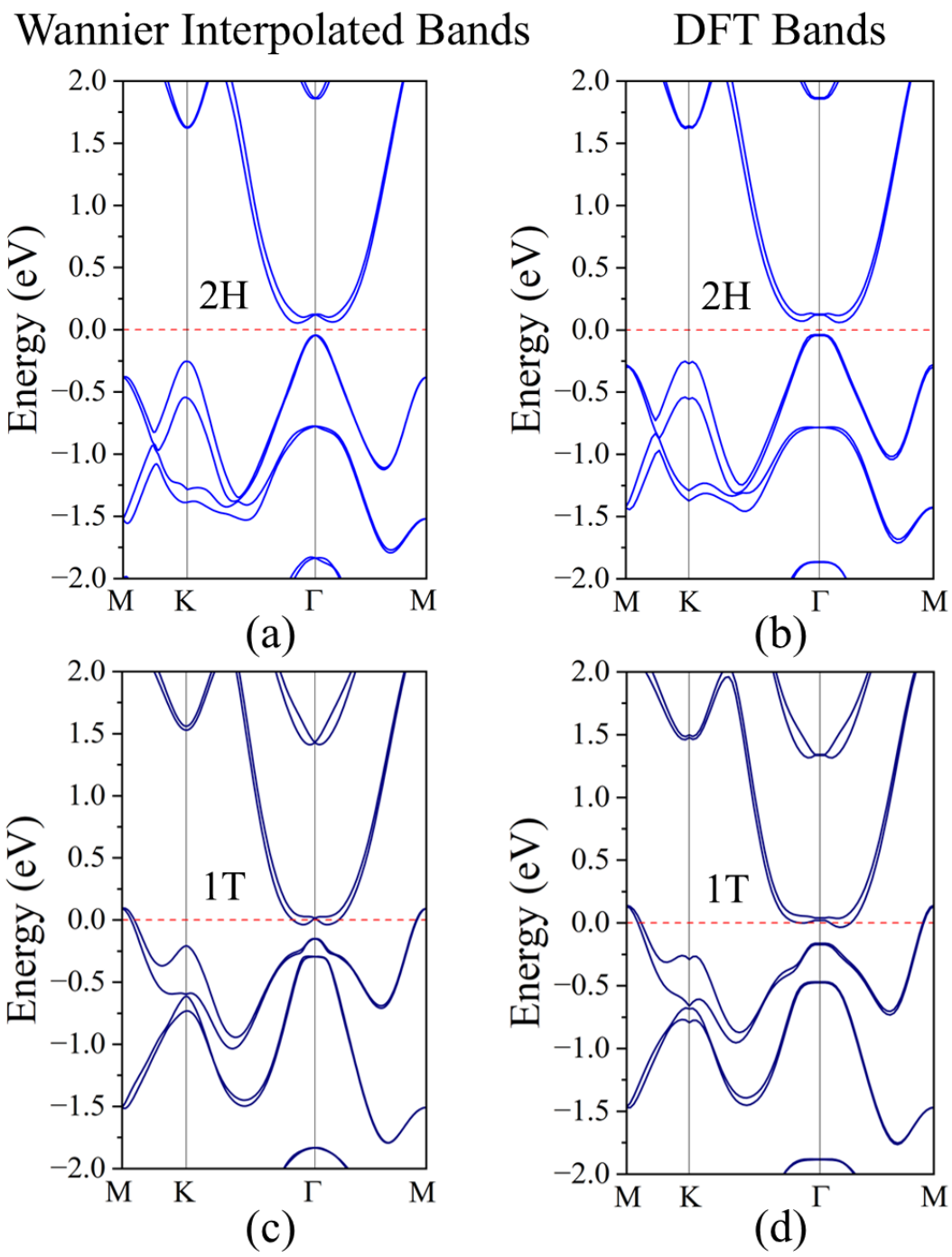

Figure S4. The Wannier-interpolated (a, c) band structures show excellent agreement with the DFT (b, d) results for Janus $MoWCO_2$ in both the 2H and 1T phases. This consistency confirms that the selected MLWF projections, *d* orbitals of Mo and W, and *p* orbitals of O and C, accurately reproduce the low-energy electronic structure, ensuring the reliability of the TB Hamiltonian used for the edge-state and Wilson-loop calculations.